Chapter 10

Pedestrian Recognition Based on 24 GHz Radar Sensors

Steffen Heuel and Hermann Rohling

Additional information is available at the end of the chapter

http://dx.doi.org/10.5772/53007

1. Introduction

Radar sensors offer in general the capability to measure extremely accurately target range, radial velocity, and azimuth angle for all objects inside the observation area. These target parameters can be measured simultaneously even in multiple target situations, which is a technical challenge for the waveform design and signal processing procedure. Furthermore, radar systems fulfil these requirements in all weather conditions, even in rain and fog, which is important for all automotive applications, [1], [2]. Advanced driver assistant systems (ADAS) are currently under investigation to increase comfort and safety in general. For Adaptive Cruise Control (ACC) applications a single 77 GHz radar sensor is used, which has a maximum range of 200 m and covers a narrow azimuth angle area of 15 degree for example. Many other and additional automotive applications, like Stop & Go, Pre-Crash or Parking Aid, consider a completely different observation area [3]. In this case a maximum range of 50 m, but a wide azimuth angle area of 120 degrees is required. For these applications 24 GHz radar sensors are used. Besides the range and velocity parameters, additional information concerning the target type are of great interest, as one of the main objectives of future safety systems will be the increased protection of all pedestrians and other vulnerable road users.

By extending the radar signal processing part of a 24 GHz radar sensor with a pedestrian recognition scheme, the same radar sensor which is used for the mentioned applications can be applied additionally for pedestrian recognition and allows the design of pedestrian safety systems. Therefore, the radar signal processing part has to be adapted to the assumption of extended targets with a characteristic range profile and a velocity profile (e.g. based on the Doppler Spectrum) in general [4]. The detailed analysis of the resulting range profile and target's velocities is possible and can be used to recognize pedestrians in urban areas with conventional 24 GHz radar sensors.

2. Radar sensor and measurements

Several proposals for pedestrian recognition schemes have been described, which are based on video cameras and computer vision systems [7], [8]. But automotive radar sensors in the

24 and 77 GHz band are also strong candidates for automotive safety systems. Compared with vision systems, they have some additional important advantages of robustness in all weather conditions, simultaneous target range and radial velocity measurement and a high update rate. These properties are especially important for pedestrian recognition, as the object classification should be available immediately and at any time.

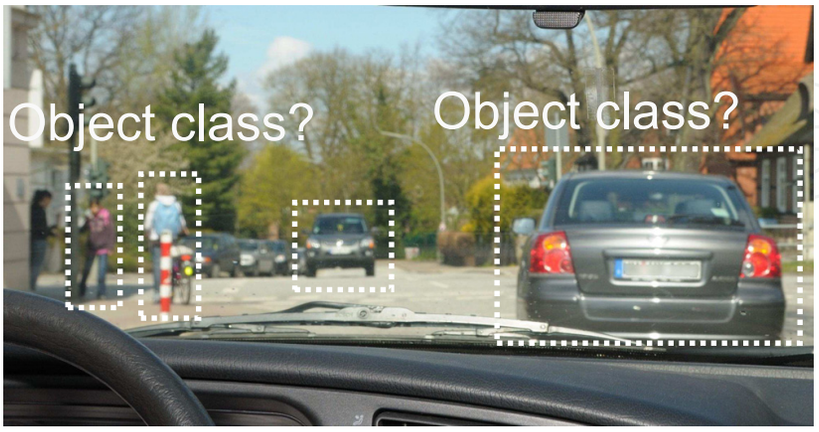

Figure 1. Daily traffic situation in an urban area with an oncoming vehicle and pedestrians walking on the sidewalk.

This chapter presents the modulation scheme of an automotive radar sensor and explains the features of pedestrians and vehicles by which a robust classification is possible in an urban area from a moving vehicle with a mounted 24 GHz radar sensor, see Figure 1.

2.1. Modulation scheme

The automotive 24 GHz radar sensor allows a simultaneous and unambiguous measurement of target range R and radial velocity v_r even in multiple target situations. This is achieved by combining the advantages of the Frequency Shift Keying (FSK) waveform and the Frequency Modulated Continuous Waveform (FMCW) in a so called Multi Frequency Shift Keying (MFSK) waveform [19], which is already used in commercial automotive radar sensors to enable Adaptive Cruise Control (ACC) or Blindspot Detection (BSD) [20], [21]. Applying an FSK waveform, the target range R and radial velocity v_r can be measured. However, there is no range resolution. Multiple objects measured at the same spectral line in the Doppler spectrum result in an unusable range information, as the determination procedure assumes a single target. To mitigate this drawback, the FMCW waveform resolves targets in range R and velocity v_r. Limitations will occur in this case in multi target situations due to ambiguous measurements. The specific MFSK waveform is applied in the 24 GHz Radar sensor for a range and Doppler frequency measurement even in multi target situations with a bandwidth of $f_\mathrm{sweep} = 150\,\mathrm{MHz}$ and a resulting range resolution of $\Delta R = 1.0\,\mathrm{m}$. It is a classical step-wise frequency modulated signal with a second linear frequency modulated signal in the same slope but with a certain frequency shift f_step integrated into this waveform in an intertwined way. The chirp duration is denoted by $T_\mathrm{CPI} = 39\,\mathrm{ms}$ which results in a velocity resolution of $\Delta v = 0.6\,\mathrm{km/h}$.

It is important to notice that this waveform is not processed by a matched filter or analyzed by an ambiguity function. Instead it is processed in a non-matched filter form to get an unambiguous and simultaneous target range and Doppler frequency measurement with

high resolution and accuracy. The echo signal of the stepwise and intertwined waveform is downconverted by the corresponding instantaneous transmit frequency into baseband and sampled at the end of each short frequency step. This time discrete signal is Fourier transformed separately for the two intertwined signals to measure the beat frequency f_B which is simultaneously influenced by the target range R and radial velocity v_r.

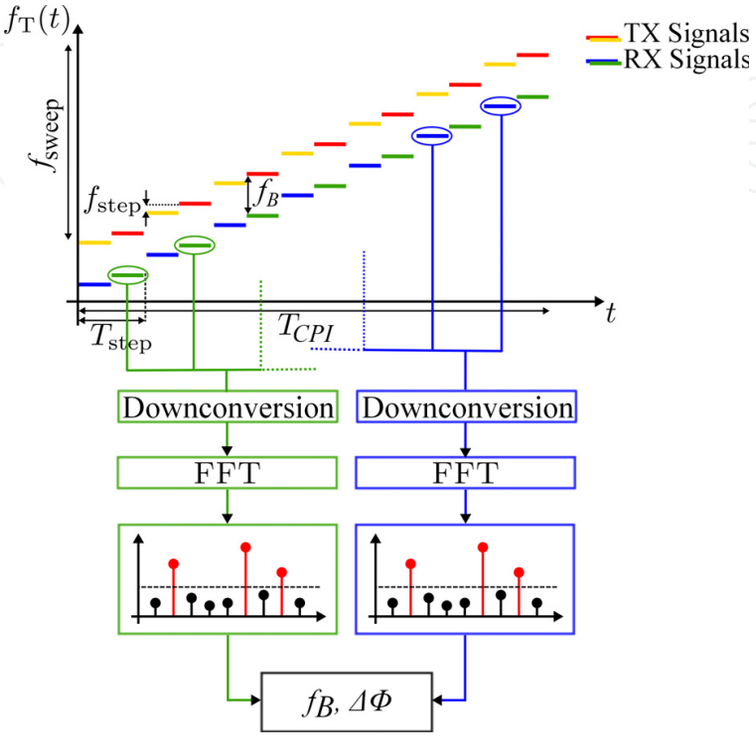

Figure 2. MFSK waveform principle with two intertwined transmit signals.

$$f_B = -\frac{2v_r}{\lambda} - \frac{2R \cdot f_{sweep}}{c} \cdot \frac{1}{T_{CPI}} \tag{1}$$

In any case, a single target will be measured and will be detected on the same spectral line at position f_B for the two intertwined signals. Therefore, after the detection procedure the phase difference $\Delta\Phi$ between the two complex-valued signals on the spectral line f_B will be calculated. The step frequency f_{step} between the intertwined transmit signals determines the unambiguous phase measurement $\Delta\Phi$ in the interval $[-\pi;\pi)$. This phase difference $\Delta\Phi$ again is influenced by the target range R and radial velocity v_r described in Equation (2).

$$\Delta\Phi = -\frac{2\pi}{f_{sample}} \cdot \frac{2v_r}{\lambda} - \frac{4\pi R \cdot f_{step}}{c} \tag{2}$$

The target range R and radial velocity v_r can be determined by solving the linear equation described in Equation (1) and (2) in an unambiguous way. In this case, ghost targets are completely avoided since this waveform and signal processing combines the benefits of linear FMCW and FSK technology. The system design and the sensor parameters can be determined like in a linear FMCW radar system. The range and velocity resolution ΔR and Δv are determined by the bandwidth f_{sweep} of the radar sensor and the chirp duration T_{CPI} as described in Equation (3) and (4), respectively.

$$\Delta R = \frac{c}{2} \cdot \frac{1}{f_{\text{sweep}}} \tag{3}$$

$$\Delta v = -\frac{\lambda}{2} \cdot \frac{1}{T_{\text{CPI}}} \tag{4}$$

The table below shows the system parameters of the automotive radar sensor in detail.

Carrier Frequency	$f_{\text{T}} = 24\,\text{GHz}$
Sweep Bandwdith	$f_{\text{sweep}} = 150\,\text{MHz}$
Maximum Range	$R_{\text{max}} = 200\,\text{m}$
Range Resolution	$\Delta R = 1\,\text{m}$
Chirp Length	$T_{\text{CPI}} = 39\,\text{ms}$
Maximum Velocity	$v_{\text{max}} = 250\,\text{km/h}$
Velocity Resolution	$\Delta v = 0.6\,\text{km/h}$

Table 1. 24 GHz Radar Sensor Parameters.

Classical UWB-Radar Sensors have a sweep bandwidth of $f_{\text{sweep}} = 2\,\text{GHz}$. Using such a bandwidth, a high range resolution is determined, which allows also pedestrian classification. The technical challenge in this chapter is to realize pedestrian recognition based on a 24 GHz radar sensor with a bandwidth of only 150 MHz. This sensor is used in automotive applications, therefore an extension of the signal processing in terms of pedestrian classification is desirable.

2.2. Radar echo signal measurements

The possibility to recognize pedestrians with a static radar sensor using the Doppler effect has been shown in [15]. A moving vehicle is equipped with an automotive radar sensor with a built-in feature extraction and classification to recognize pedestrians. The feature extraction in the backscattered radar echo signals resulting from superposition of the reflection points of an object is done automatically in the radar sensor signal processing. Detected targets are therefore tracked in the environment and an additional feature extraction and classification is performed.

To distinguish between the echo signal characteristics of pedestrians and vehicles, a target recognition model is described which is based on the specific **velocity profile** and **range profile** for each object separately [4]. The velocity profile describes the extension of the different velocities of an object measured by the radar sensor, while the range profile shows the physical expansion of a target.

In case of a longitudinally moving pedestrian, different reflection points at the trunk, arms and legs with different velocities are characteristic in radar propagation. Therefore an *extended* velocity profile will be observed in a single radar measurement of a pedestrian as the velocity resolution Δv of the radar sensor is higher than the occuring velocities. Carrying out several measurements with a time duration of 39 ms each, a sinusoidal spreading and contraction of the velocity profile can be observed in the case of a pedestrian, due to the movement of arms and legs for example in the swing and stand-phase of the legs. For a laterally moving

pedestrian, the velocity profile is less extended due to the moving direction of the pedestrian. Furthermore, the extension depends mainly on the azimuth angle under which the pedestrian is measured. In contrast, the radar echo signal in case of a vehicle shows a very narrow (*point shaped*) velocity profile due to a uniform motion.

Additionally, a *point shaped* range profile will occur in the case of a longitudinally or laterally moving pedestrian as the physical expansion is small compared to the range resolution of $\Delta R = 1.0\,\text{m}$. In contrast, a vehicle shows an *extended* range profile, due to several reflection points spaced in several range cells. The measurement result of a single observation is shown in the range Doppler diagram in Figure 4.

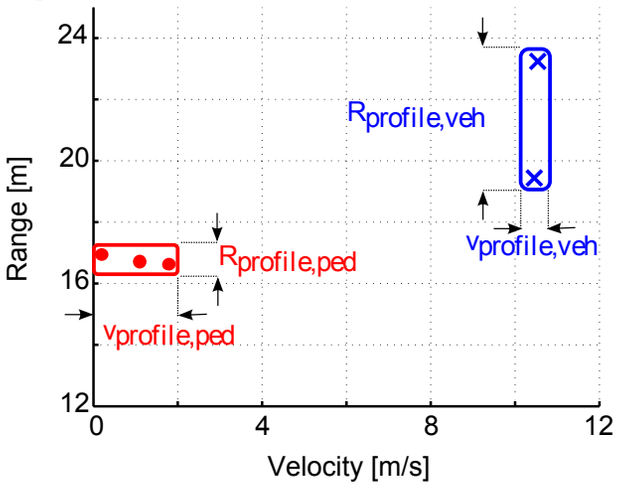

Figure 3. Range profile and velocity profile of a single measurement.

Under the use of an MFSK modulation signal, a range profile and the velocity profile can be extracted from a series of received signals as shown in Figure 4. As an example, four consecutive range and velocity measurements are depicted in a range Doppler diagram. The red dots show a longitudinally walking pedestrian, the blue crosses an in front moving vehicle. The figures depicted are based on radar measurements taken in an urban area with an ego speed of 50 km/h. It can be observed that neither velocity profile nor a range profile can be seen in the first measurement, consequently, those feature values are zero. In the second measurement, however, several range and velocity measurements allow to calculate an extended range profile for the vehicle and an extended velocity profile for the pedestrian.

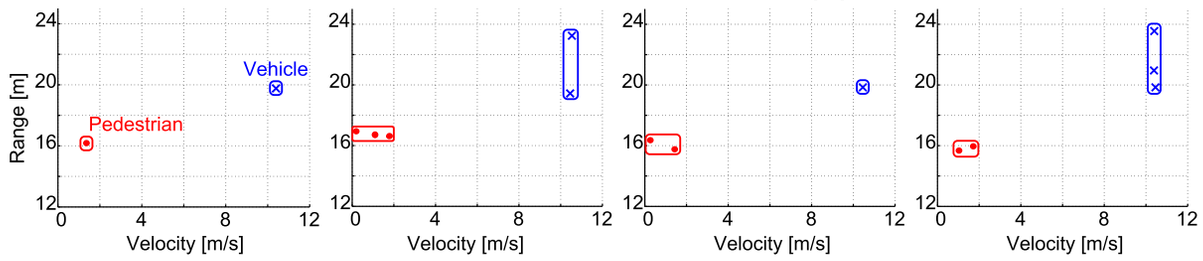

(a) Measurement 1 (b) Measurement 2 (c) Measurement 3 (d) Measurement 4

Figure 4. Sequence of range and velocity measurements.

The range profile and velocity profile features do not depend on the modulation signal. Solely, the range and velocity resolution must be smaller than the expected extension. For example, in the case of a continous wave modulation signal, the range profile can be read directly from the Fourier transformed radar echo signal and the velocity profile can be evaluated from the Doppler spectrum. Also, instead of these spectra or the frequency spectrum and phase difference analysis, it is possible to calculate the extension of an object in range and velocity on the basis of target lists by applying a detection algorithm. On this basis, an extended range profile with a point-shaped velocity profile can also be measured for a vehicle. For a pedestrian, the profiles remain vice versa. Figure 5 depicts this context.

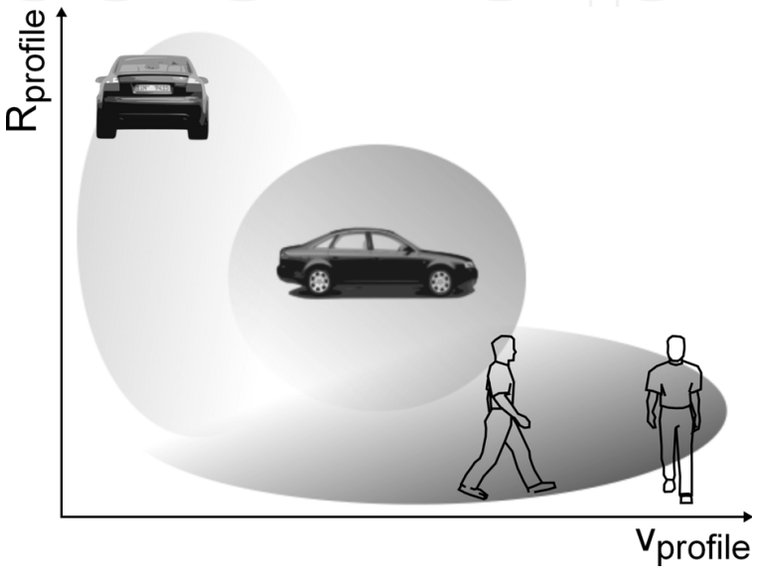

Figure 5. Range profile and velocity profile of a pedestrian and a vehicle.

The longitudinally and laterally moving pedestrians are classified as **pedestrians**, longitudinally and laterally moving vehicles as **vehicles**, all other signals received from objects such as parked cars, poles, trees and traffic signs are classified as **other** objects.

3. Classification

Target recognition is a challenge for each radar engineer. A reliable feature extraction and classification process has to be implemented. To describe the characteristics of pedestrians and vehicles, the velocity profile and range profile signal features have been introduced. These are the basis in the feature extraction and target recognition system based on a single radar measurement (single look of 39 ms duration) as described in subsection 3.1. An extended extraction based on the spreading and contraction of the spectra by observing several measurements is considered in subsection 3.2. Finally in subsection 3.3, a tracker feedback is calculated where additional features based on the Kalman gain and innovation are extracted. In the next step, the classification process is performed, which maps the extracted features into classes. An evaluation of the classification results is shown by means of a confusion matrix for the case of a single measurement- and multiple measurements-feature extraction.

3.1. Classification based on a single radar measurement

Radar sensors provide continuously available measurement results in an interval of a few milliseconds. This interval is determined by the duration of the transmission signal $T_{\mathrm{CPI}} = 39\,\mathrm{ms}$ in which a single MFSK signal is transmitted. The echo signal is downconverted and Fourier-transformed, which allows the described features to be extracted continuously. Rather than examinating a received sequence of radar echoes, this subchapter will initially focus on a single radar measurement of $T_{\mathrm{CPI}} = 39\,\mathrm{ms}$.

3.1.1. Feature extraction

Automotive radar sensors are an important source of information for security and comfort systems. The information is measured in terms of range, radial velocity and signal level. However, information about the object types do not exist. To fill this gap, features from the available information are extracted, which describe the object types and allow a decision of the related class on the basis of measured sensor data. To describe a detected object, this signal processing step calculates a number of features, which are discriminant for measurements containing different object types and match for objects from the same type. Thereby, moderately separated features achieve even in a perfect classification algorithm only moderate or even poor results ([16], [17]). An ideal feature extractor on the other hand shows good classification performance by using simple linear classifiers. This is why the feature extraction is so important. For a distinct classification, transformation-invariant features are sought. Still, there is no recipe to determine a feature set and since each sensor type describes an object specifically and each task is different, the feature set for pedestrian recognition based on an automotive radar sensor is explained shortly. Figure 6 shows the feature extraction with the specific object description in the context of the signal processing chain.

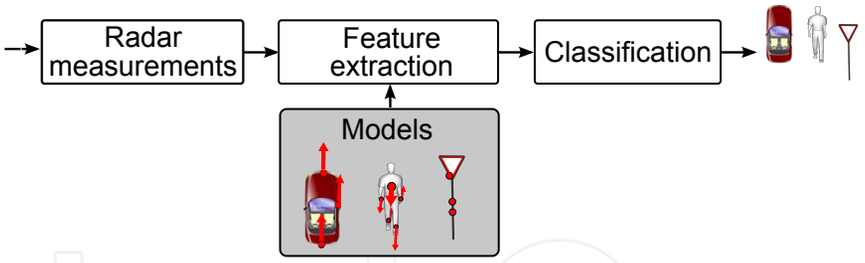

Figure 6. Context of the feature extraction in the signal processing chain and the object description using the range profile and velocity profile.

The basis for feature extraction are the velocity profile and the range profile of a detected object which has been described previously. The term of the profile describes the physical and kinematic dimensions of an object in the distance, angle and velocity. This can be measured in the case of multiple reflection points with different velocities greater than zero for any object. It can involve an extended or a point-shaped profile for the range and velocity depending on the type of expansion. On this basis, a number n of features can be calculated which describe the object in terms of a radar measurement. All n calculated real valued features $x_1, ..., x_n$ are saved in a feature vector $\vec{x}$ and build the basis for further signal processing steps.

$$\vec{x} = (x_1, x_2, ..., x_n)\ n \in \mathbf{N}, x_{\mathrm{i}} \in \mathbf{R} \tag{5}$$

Exemplarily, the calculation of the range profile R_{profile} is given in Equation (6). Analogously, the velocity profile v_{profile} of the spectrum can be calculated, Equation (7).

$$x_1 = R_{\text{profile}} = R_{\text{max}} - R_{\text{min}} \tag{6}$$

$$x_5 = v_{\text{profile}} = v_{\text{max}} - v_{\text{min}} \tag{7}$$

The approach in feature extraction, using stochastic features, assumes that the measured data are random variables with independent and identical distribution. From this data within a single measurement cycle the variance and the standard deviation is estimated. To support the classification process, the number of scatterers is extracted, which describes the number of detected reflection points of an object. This approach allows a classification of the object type within a single measurement. The entire feature set for $n = 8$ features is shown in Table 2 below.

Feature	Annotation	Description
x_1	R_{profile}	Extension in range
x_2	$std(R)$	Standard deviation in range
x_3	$var(R)$	Variance in range
x_4	v_{r}	Radial Velocity
x_5	v_{profile}	Extension in velocity
x_6	$std(v_r)$	Standard deviation in velocity
x_7	$var(v_r)$	Variance in velocity
x_8	scatterer	Number of scatterers

Table 2. Feature Set of each object in a single measurement.

To determine the quality of a feature, the common area index (CAI) of two histograms is considered. While a common area index of 0 describes a complete overlapping of the feature space, a CAI of 1 describes an absolutely separable feature.
Several urban measurement scenarios of longitudinally moving vehicles and pedestrians were measured with an automotive radar sensor. From the detections of each single measurement cycle the features are extracted. Exemplarily, the velocity profile of a vehicle and a pedestrian is depicted in Figure 7 as a histogram. It shows a strong overlap of the area with a point shaped extension. This results directly from the model. A pedestrian is not extended at all times, because the arms and legs move sinusoidally. In addition, the echo signal fluctuates which causes fewer detections in a measurement. The vehicle equipped with the radar sensor moves also. The quality of the feature is calculated to CAI = 0.57.

3.1.2. Classification

The assignment of a measured object to a class is performed by a subjective decision algorithm based on the extracted characteristics. This process is called classification. The features therefore have been described previously, and are extracted within a single radar measurement of $T_{\text{CPI}} = 39$ ms. In supervised classifiers, the model of the classifier is generated in a training phase by using a training data set. The verification is performed in an evaluation phase with a test data set. The training data and test data consist of randomly selected feature vectors $\vec{x}$ of the radar measurements and corresponding assigned class labels. In the training and evaluation phase the classification result can be compared to the class labels and make a

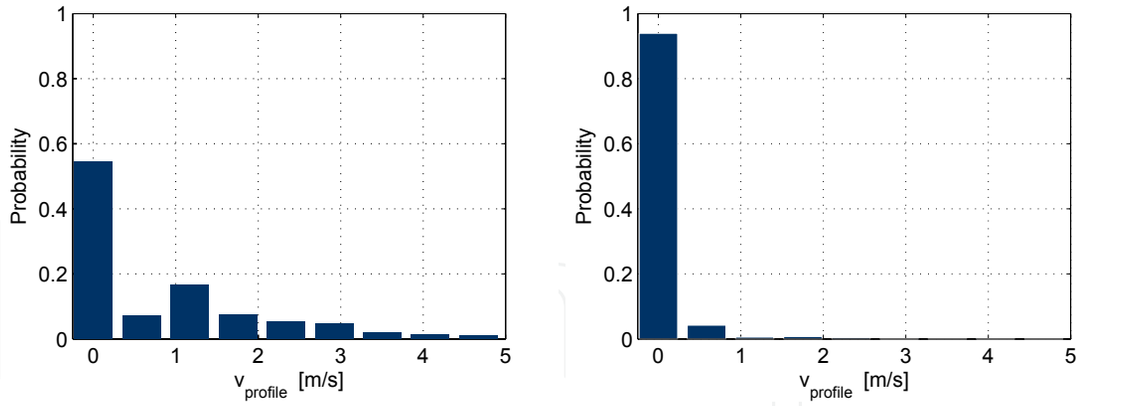

(a) v_{profile}, Pedestrian (b) v_{profile}, Vehicle

Figure 7. Feature histogram of the velocity profile using single radar measurements as a basis for feature extraction. The common area index is calculated to 0.57.

statement about the performance of the algorithm and designed model. Figure 8 depicts this process.

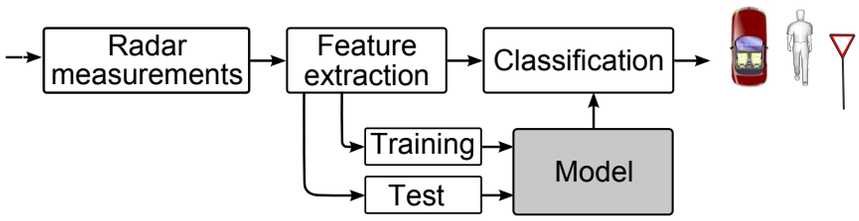

Figure 8. Signal flow graph of the classification process. Using a training data-set a model can be evaluated which performance is measured by a labelled test data set. This model is used for the classification process.

A classifier based on statistical learning theory is the support vector machine (SVM), introduced by Boser et al. in 1992 [24]. The SVM became very famous as studies about classification algorithms show good performance [25]. The classification process has low complexity and is very effective for high dimensional feature vectors. An SVM separates a set of training data by calculating a hyperplane $h(x)$ with maximum margin between the two classes ± 1 in a higher dimensional space in order to find the best classification function.

In this classification process, the SVM is able to map the extracted feature set into three different classes by using a majority voting algorithm. The verification of the previous training is conducted with the help of test data sets recorded from real urban measurements.

Table 3 shows the classification results. A trained and tested SVM was applied to different data sets of the extracted features from single measurements. All measurements were taken in an urban area with an ego velocity of 50 km/h. Applying new test data results in 71.32% true positive for a vehicle and 45.20% true positive for a pedestrian.

These quantitative results show already a possibility to distinguish between vehicles, pedestrians and other objects. However the performance is not good enough. Therefore

	Vehicle	Pedestrian	Other
Vehicle	71.32	5.87	22.81
Pedestrian	10.29	45.20	44.52
Other	23.56	26.65	49.78

Table 3. Confusion matrix: classification applied to a single measurement test data set containing 8000 data samples.

multiple radar measurements are considered to extract a more significant features set for the classification process.

3.2. Classification based on multiple radar measurements

From the continuously available radar measurements, a single measurement can be used to extract a feature set on the basis of range profile and velocity profile and estimated stochastic features. In this section, several range and velocity measurements are buffered and build the basis for the additional extraction process. From these buffered measurements a second **multiple measurement feature set** is extracted. This extends the classification process, which was previously based on a single measurement only.

3.2.1. Feature extraction

To gain performance, the choice of the measurement buffer dimension is cruical. A long measurement buffer builds the basis for a more successful feature extraction, however results in a long classification time, as the classifier has to wait for the buffer to be filled. A short buffer, on the other hand is not always able to build the basis for separable features, as shown in the previous section where a single measurement is used. In this section, the dimension of the buffer is explained by means of "probability of maximum velocity profile" and fast availability deduced from the step frequency of a moving pedestrian.

An ideal measurement of a moving pedestrian allows to extract the step frequency from the spreading and contraction of the velocity profile [9]. This step frequency of $f_{\text{ped}} = 1.4 - 1.8\,\text{Hz}$ can be used to determine a necessary buffer dimension. Every 1.4 Hz the maximum velocity profile can be observed considering a moving pedestrian, which allows to extract the maximum velocity profile and range profile. At all other times, the expansion in velocity is lower or even zero. To detect at least one expansion in velocity, the number of measurements should therefore span a period of $T_{\text{ped}} = \frac{1}{f_{\text{ped}}}$. However, it can be assumed that all measurements are independent of each another, due to the ego motion of the radar, vibrations and fewer detections. Applying the feature extraction process using a single measurement, the probability P to extract an extended velocity is then given by:

$$P_{v_{\text{profile}},\text{single}} = \frac{T_{\text{CPI}}}{1/f_{\text{ped}}} \tag{8}$$

Assuming an equal distribution, multiple measurements increase the probability to extract a velocity profile by the factor $\frac{T_{\text{Buffer}}}{T_{\text{CPI}}}$.

$$P_{v_{\text{profile}},\text{multiple}} = \frac{T_{\text{Buffer}}}{T_{\text{CPI}}} \cdot \frac{T_{\text{CPI}}}{1/f_{\text{ped}}} \tag{9}$$

It can be seen that a long measurement buffer increases the probability to detect the maximum velocity profile. But even a smaller velocity profile can be detected and fulfils the requirements. In these measurements, a buffer of $T_{\text{Buffer}} = 150\,\text{ms}$ is applied.

Using current and time delayed range measurements leads to incorrect range profiles, due to the movement of the objects during the elapsed buffer time. To cope this, the corresponding range measurements inside the buffer must therefore be predicted in range. Each stored measurement is predicted in range by the elapsed time ΔT_{Buffer} and the velocity $\vec{v} = (v_{\text{x}}, v_{\text{y}})$ during the measurements to compensate the movement. A new estimated range $\widehat{R} = |\vec{R^*}|$ can be calculated by a cartesian representation using velocity and elapsed time:

$$\vec{R^*} = \vec{R} + \Delta T_{\text{Buffer}} \cdot \vec{v} \text{ with } \vec{R} = (X, Y) \text{ and } \vec{v} = (v_{\text{x}}, v_{\text{y}}) \tag{10}$$

The multiple measurement feature set is shown in Table 4. It consists of the same characteristics as the single measurement feature set, but is calculated from a basis of several buffered velocity and predicted range measurements.

Feature	Annotation	Description
x_9	$\widehat{R}_{\text{profile,buf}}$	Extension in range
x_{10}	$std(\widehat{R}\text{,buf})$	Standard deviation in range
x_{11}	$var(\widehat{R}\text{,buf})$	Variance in range
x_{12}	$v_{\text{r,buf}}$	Radial Velocity
x_{13}	$v_{\text{profile,buf}}$	Extension in velocity
x_{14}	$std(v_{\text{r,buf}})$	Standard deviation in velocity
x_{15}	$var(v_{\text{r,buf}})$	Variance in velocity
x_{16}	scatterer,buf	Number of scatterers

Table 4. An additional feature set extracted from multiple measurements. To cover multiple measurements, each single measurement R, v_{r} is stored in a buffer of several milliseconds. This ensures a quick availability of an additional feature set for pedestrian classification.

In the previous section the characteristic velocity profile of a vehicle and a pedestrian was depicted as a histogram. On the basis of a single radar measurement a quality of CAI $= 0.57$ was determined. Using multiple radar measurements the feature extraction is based on a larger number of measurement values. This leads to a higher separability of the features as shown exemplarily in Figures 9(a), 9(b). The common area index has a value of CAI $= 0.88$ and thus increases by 31% compared to the single measurement feature extraction.

3.2.2. Classification

In the single measurement it is described how range and velocity measurements build the basis for the feature vector and the classification process. In the multiple measurement, the basis is an extended feature vector based on several range and velocity measurements of an object stored inside a buffer. Instead of using 8 features from a single measurement, additional 8 features are available for the first time with a filled buffer. For a successful classification using a SVM, a new model is built, which is also trained/tested with in total 16 features and is a basis for the following classification process. As shown in the confusion matrix in Table 5 by the additional features, the correct classification and the overall performance achieved, increases by using a total number of 16 features from single and multiple measurements.

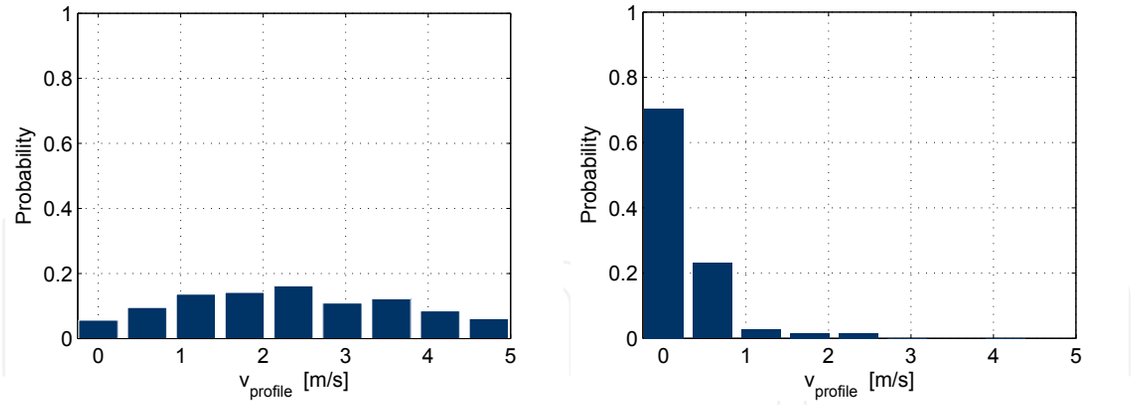

(a) $v_{\text{profile,buf}}$, Pedestrian (b) $v_{\text{profile,buf}}$, Vehicle

Figure 9. Feature histogram of the velocity profile using multiple radar measurements as a basis for feature extraction. The common area index is calculated to 0.88.

Additionally, classifying feature vectors from single and multiple measurements results in fewer false positives.

	Vehicle	Pedestrian	Other
Vehicle	90.71	0.58	8.71
Pedestrian	4.94	53.94	41.12
Other	16.28	16.64	67.08

Table 5. Confusion matrix: classification applied to a single and multiple measurement test data set containing 8000 data samples.

Due to additionally multiple measurements as a basis for feature extraction, an improvement in the classification result is shown. Especially in terms of correct classification of a pedestrian and false alarms in which a pedestrian was classified as a vehicle, a significant enhancement is seen.

3.3. Classification based on the tracker feedback

A single radar measurement and multiple radar measurements were considered for feature extraction. These features are already a good basis for the classification process. In this subchapter, a third, additional feature set is described. This set can be extracted from the tracking algorithm. In this adaptive algorithm, different process noise of pedestrian radar measurements and vehicle radar measurements result in different gains for the track. On this basis, the process noise Q and the calculated gain K are additional features and are added to single and multiple radar measurement features in the classification process.

3.3.1. Feature extraction

Tracking is defined by a state estimation of moving targets. This state estimation is determined from the state parameters such as position, velocity and acceleration from a detected target. Known tracking methods are for example the alpha-beta filter or Kalman filter [26] which

estimate a new state using a well-known prior state (e.g. position, velocity, acceleration). This reduces false alarms and smoothes movements of the objects.

The Kalman filter is a linear, recursive filter, whose goal is to determine an optimal estimate of the state parameters. The optimal estimate is based on available measurements and the models which describe the observed objects. In the equation of the motion model and observation model, the measurement noise is assumed to be average free, white Gaussian noise with the known covariance Q_{k-1} and R_k respectively. Under the given conditions, i.e., linear models and Gaussian statistics, the Kalman filter provides the optimal solution for the estimation of the state in the sense of minimizing the mean squared error, as described in [26].

The tracking for the object described by the motion model of the Kalman filter works fine as long as the motion models fit to the object. Pedestrians, vehicles, and static objects have different motion, which makes the tracking more difficult. Instead of creating a different motion and observation model for each object, it is proposed to determine the covariance of process noise Q_k and the measurement noise R_k adaptively. The process noise considers a non-modeled behavior in the motion model, while the measurement noise consideres uncertainty in the measurement. The original Kalman filter is not adaptive, which is why deviations from the model can not be handled. The gain matrix K, which is calculated from the process and measurement noise, reaches a stable condition after a short measurement time. An increase in the covariance Q_k leads to a larger value for K, so that the measured values are weighted more strongly, a decrease in Q_k relies more on the estimation.

In addition to an improved tracking effect, additional features can be extracted from the adaptive adjustment of the process noise, as pedestrian measurements in range and velocity differ from those of vehicles. Next to the process noise $Q_{k,v}$ of the velocity, the Kalman gain K_v (velocity component of the matrix K) is a good feature as measurements show. Anyhow, in an adaptive adjustment of the process noise, a compromise between the compensation of non-modeled movements and the filtering effect to reduce noise must be found, even though features are extracted.

The process noise matrix Q describes object-specific measurement properties that are initially set and are readjusted during operation of the tracker. For example, the readjustment of a single coefficient $Q_{k,v}$ in the Q matrix at the measurement k in respect to the velocity v is based on the actual target range R, the velocity v, the parameters a and b in an alpha-beta filter. Equation (11) shows the relation. The velocity of a pedestrian deviates between consecutive measurements, while the velocity deviation of a car within consecutive measurements is small or even zero. Consequently, the velocity v can be used to update the matrix Q.

$$Q_{k,v} = (1-\beta)Q_{k-1,v} + \beta\frac{|z_{k,v} - v_{k|k-1}|}{R_{k|k} \cdot a + b} \tag{11}$$

The predicted covariance matrix $P_{k|k-1}$ in the tracking process depends on the motion model F_{k-1}, the currently measured covariance $P_{k-1|k-1}$ and the process noise Q_{k-1} as shown in Equation (12).

$$P_{k|k-1} = F_{k-1}P_{k-1|k-1}F_{k-1}^T Q_{k-1} \tag{12}$$

Under the use of this covariance matrix $P_{k|k-1}$ and the innovation covariance S_k, the gain K_k can be calculated.

$$K_k = P_{k|k-1} S_k^{-1} \tag{13}$$

Both, matrix Q_k and gain K_k are used as additional features in the classification process. The separation of the feature space is depicted in Figure 10. These histograms show that a vehicle (Figure 10(c), 10(d)) has lower process noise Q_v and thus results in a smaller gain K compared to a pedestrian (Figure 10(a), 10(b)). This is due to a mostly linear trajectory of a vehicle with one main reflection point. A pedestrian echo fluctuates, which is reflected in a greater process noise and thus larger gain K.

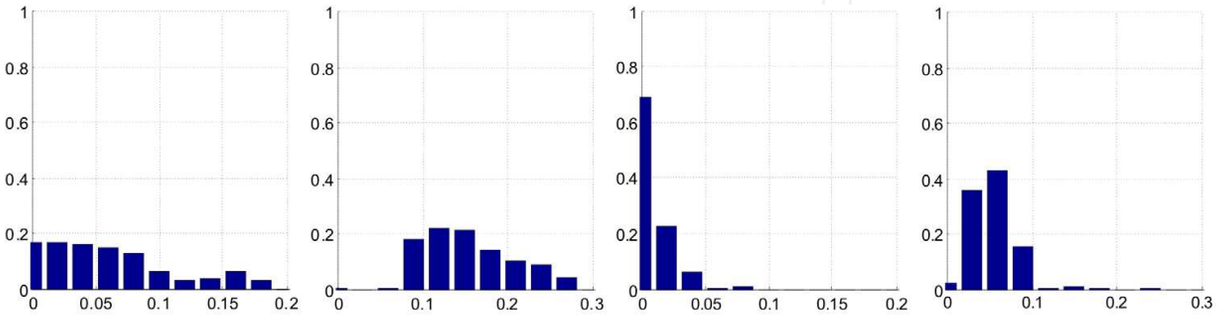

(a) Q_v, Pedestrian (b) K, Pedestrian (c) Q_v, Vehicle (d) K, Vehicle

Figure 10. Feature Histogram of Process Noise Q_v and Gain K.

The additional features Q and K are available for a created and active track. For each detected object a track is created, which is however not activated until several measurements can be associated with the track. A track must be confirmed by subsequent measurements, otherwise the track remains semi-active. In any case, additional features are available for classification.

Feature	Annotation	Description
x_{17}	Q_v	Velocity component of the process noise matrix Q
x_{18}	K_v	Veleocity component of the Kalman gain matrix K

Table 6. Additional Feature Set extracted from the tracker using an adaptive process noise.

3.3.2. Classification

An additional feature extraction based on the process noise and Kalman gain has been described. These features are added to the prior feature set. Table 7 shows the results of the classifier using all proposed features, single measurement, multiple measurements and tracker feedback. Even in an urban area with a high density of static targets pedestrians could be detected, tracked and classified with a true positive rate of 61.22% in the test data set. These results outperform prior outcomes using single- and the multiple measurements as a feature basis.

The classification results show an increasing performance in terms of correct classification and misclassification of pedestrians.

	Vehicle	Pedestrian	Other
Vehicle	92.84	0.50	6.66
Pedestrian	5.71	61.22	33.07
Other	10.06	13.30	76.64

Table 7. Confusion matrix: classification applied to a single, multiple and tracker feedback measurement test data set containing 8000 data samples.

4. Summary and conclusions

This chapter described a pedestrian classification algorithm for automotive applications using an automotive 24 GHz radar sensor with a bandwidth of 150 MHz as a measuring device. Three different systems for pedestrian recognition have been considered. The first system was based on a single radar measurement. The second system extracted a feature set on the basis of multiple radar measurements. Finally a tracking procedure was adapted to extract an additional feature set. The results show an increasing performance in the classification accuracy by using single-, multiple- and tracker feedback features. It is also pointed out that is not necessary to equip radar sensors with large bandwidths in order to classify pedestrians in urban areas.

Author details

Hermann Rohling and Steffen Heuel
Department of Telecommunications, Hamburg University of Technology, Hamburg, Germany

5. References

[1] Foelster, F.; Oprisan, D.; Rohling, H., (2004) Detection and Tracking of extended targets for a 24GHz automotive radar network, International Radar Symposium IRS 2004, Warsaw, Poland; pp 75-80
[2] Meinecke, M.-M.; Obojski, M.; Toens, M.; et.al, (2003) Approach For Protection Of Vulnerable Road Users Using Sensor Fusion Techniques, International Radar Symposium IRS 2003, Dresden, Germany, pp 125-130
[3] Schiementz, M.; Foelster, F. (2003) Angle Estimation Techniques for different 24 GHz Radar Networks, International Radar Symposium IRS 2003, Dresden, Germany, 2003
[4] Rohling, H.; Heuel, S.; Ritter, H. (2010) Pedestrian Detection Procedure integrated into an 24 GHz Automotive Radar, IEEE RADAR 2010, Washington D.C.
[5] Schmid, V.; Lauer, W.; Rollmann, G. (2003) Ultra Wide Band 24 GHz Radar Sensors for Innovative Automotive Applications, International Radar Symposium IRS 2003, Dresden, Germany, pp 119-124
[6] Oprisan, D.; Rohling, H.,(2002) Tracking Systems for Automotive Radar Networks, IEE Radar 2002, Edinburgh
[7] Philomin, V.; Duraiswani, R.; Davis, L. (2000) Pedestrian tracking from a moving vehicle, Proceedings of the IEEE Intelligent Vehicle Symposium 2000, Dearborn (MI), USA
[8] Ran, Y. et al (2005) Pedestrian classification from moving platforms using cyclic motion pattern, IEEE International Conference on Image Processing 2005, Volume 2, pages: II 854-7

[9] Van Dorp, P.; Groen, F. (2003) Real-Time Human Walking Estimation with Radar, International Radar Symposium IRS 2003, Dresden, Germany, pp 645-650
[10] Lei, J.; Lu, C. (2005) Target Classification Based on Micro-Doppler Signatures, IEEE International Radar Conference 2005; Arlington, USA; pp 179-183
[11] Klotz, M. (2002) An Automotive Short Range High Resolution Pulse Radar Network, Phd. Thesis, Hamburg University of Technology, Hamburg, Germany
[12] Luebbert, U. (2005) Target Position Estimation with a Continuous Wave Radar Network, Phd. Thesis, Hamburg University of Technology, Hamburg, Germany
[13] Foelster, F., Rohling, H. and Meinecke, M. M. (2005) Pedestrian recognition based on automotive radar sensors, 5th European Congress on Intelligent Transportation Systems and Services 2005, Hannover, Germany
[14] Heuel, S.; Rohling, H. (2011) Two-Stage Pedestrian Classification in Automotive Radar Systems, International Radar Symposium IRS 2011, Leipzig, Germany
[15] Nalecz, M.; Rytel-Andrianik, R.; Wojtkiewicz, A. (2003) Micro-doppler analysis of signals received by FMCW radar, Proceedings of International Radar Symposium 2003, Dresden, Germany, pp. 651-656
[16] Duda, R. O.; Hart, P. E.; Stork, D. G. (2001) Pattern classification, Wiley, New York
[17] Schuermann, J. (1996) Pattern Classification - A Unified View of Statistical and Neural Approaches, Wiley, New York
[18] Schiementz, M. (2005) Postprocessing Architecture for an Automotive Radar Network, Phd. Thesis, Hamburg University of Technology, Hamburg, Germany
[19] Meinecke, M.-M.; Rohling, H. (2000) Combination of LFMCW and FSK modulation principles for automotive, German Radar Symposium GRS 2000, Berlin, Germany
[20] Winner, H., Hakuli, S., Wolf, G., (2009), Handbuch Fahrerassistenzsysteme, Vieweg+Teubner Verlag / GWV Fachverlage GmbH, Wiesbaden, Germany
[21] Smart Microwave Sensors GmbH, (2012), UMRR | LCA BSD Technical Information Sheet, available at http://www.smartmicro.de/images/stories/contentimage/automotive/LCA and BSD Technical Information.pdf, Accessed: 30 August 2012
[22] Perry, J. (1992) Gait Analysis - Normal and Pathological Function, SLACK Incorporated, ISBN 1556421923
[23] Foelster, F.; Ritter, H., Rohling, H. (2007) Lateral Velocity Estimation for Automotive Radar Applications, The IET International Conference on Radar Systems, Edinburgh, Great Britain
[24] Boser, B. E.; Guyon, I. M.; Vapnik, V. N. (1992) A training algorithm for optimal margin classifiers, In D. Haussler, editor, 5th Annual ACM Workshop on COLT, Pittsburgh, PA, pp. 144-152
[25] Wu, X.; Kumar, V.; Ross Quinlan, J.; Ghosh, J.; Yang, Q.; Motoda, H.; McLachlan, G. J.; Ng, A.; Liu, B., Yu, P. S. and others (2008) Top 10 algorithms in data mining, Knowledge and Information Systems, Vol. 14, No. 1., pp. 1-37
[26] Branko, R.; Sanjeev, A.; Nei, G. (2004) Beyond the Kalman Filter: Particle Filters For Tracking Applications, Artech House Inc.